Research on Engineering Structures & Materials
www.jresm.org
Research Group

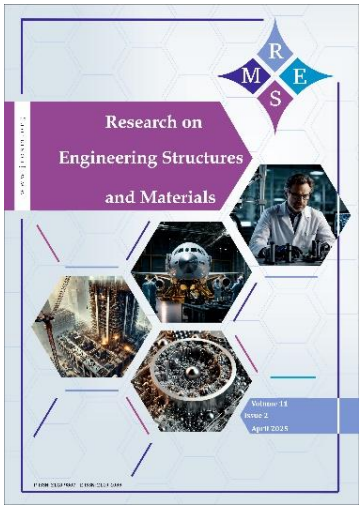

Multi-mode material response of basalt- and glass-fiber-reinforced dense-graded asphalt

Lamya M. J. Mahdi, Sozan S. Rasheed, Mohammed Y. Fattah

Online Publication Date: 10 October 2026

URL: http://www.jresm.org/archive/resm2026-2225ma0819rs.html
DOI: http://dx.doi.org/10.17515/resm2026-2225ma0819rs

Journal Abbreviation: *Res. Eng. Struct. Mater.*

To cite this article
Mahdi L M J, Rasheed S S, Fattah M Y. Multi-mode material response of basalt- and glass-fiber-reinforced dense-graded asphalt. *Res. Eng. Struct. Mater.*, 2026; 12(5): 4271-4282.

Disclaimer
All the opinions and statements expressed in the papers are on the responsibility of author(s) and are not to be regarded as those of the journal of Research on Engineering Structures and Materials (RESM) organization or related parties. The publishers make no warranty, explicit or implied, or make any representation with respect to the contents of any article will be complete or accurate or up to date. The accuracy of any instructions, equations, or other information should be independently verified. The publisher and related parties shall not be liable for any loss, actions, claims, proceedings, demand or costs or damages whatsoever or howsoever caused arising directly or indirectly in connection with use of the information given in the journal or related means.

Published articles are freely available to users under the terms of Creative Commons Attribution - NonCommercial 4.0 International Public License, as currently displayed at here (the “CC BY - NC”).

Research on Engineering Structures & Materials
www.jresm.org
MIM Research Group

Research Article

Multi-mode material response of basalt- and glass-fiber-reinforced dense-graded asphalt

Lamya M. J. Mahdi [*,a], Sozan S. Rasheed [b], Mohammed Y. Fattah [c]

Department of Highway and Geotechnical Engineering, College of Civil Engineering, University of Technology, Baghdad, Iraq

Article Info

Article History:

Received 19 Aug 2026

Accepted 01 Oct 2026

Keywords:

Basalt fiber;
Glass fiber;
Hot mix asphalt;
Wheel tracking;
Fatigue;
Cantabro abrasion

Abstract

Short mineral fibers can modify load transfer across several asphalt damage modes, but direct comparisons within one controlled mixture matrix remain limited. This study compared 6 mm basalt fiber (BF) and glass fiber (GF), incorporated by the dry process at 0.2%, 0.3%, and 0.4% of the total mixture mass, in dense-graded hot-mix asphalt prepared with a 60/70 penetration-grade binder at a fixed asphalt content of 5.0% by total mixture mass. Marshall response along with dry and moisture-conditioned indirect tensile strength was first used to examine dose dependence and select a common dosage for further testing. The 0.3% mixtures were then evaluated by wheel tracking at 60 °C, constant-strain four-point bending fatigue, and an adapted Cantabro abrasion procedure before and after thermal aging. Both fibers produced a non-monotonic load-capacity response, and 0.3% was selected for the extended test program based on the combined Marshall and tensile response within the evaluated dosage range. At this dosage, BF and GF increased Marshall stability by 27.2% and 17.5%, increased dry tensile strength by 15.5% and 11.9%, and reduced rut depth after 10,000 wheel passes by 30.0% and 22.9%, respectively. Fatigue life increased by 49.1% and 46.3%. After seven days of aging at 60 °C, Cantabro mass loss decreased from 27.0% for the control to 15.1% for BF and 18.3% for GF. Across the evaluated laboratory response modes, BF showed larger numerical improvements in several indicators, particularly rut depth and aged particle loss.

© 2026 MIM Research Group. All rights reserved.

1. Introduction

Hot mix asphalt (HMA) is a heterogeneous, temperature- and loading-rate-dependent composite in which a mineral skeleton is embedded in a viscoelastic binder in a rich mastic and interrupted by air voids. Its macroscopic response emerges from aggregate contact forces, binder rheology, mastic cohesion, aggregate-binder adhesion, and void structure. Temperature, loading duration, water, and oxidative aging all affect how stress and strain are partitioned among these phases. Rutting, fatigue cracking, moisture-related damage, and raveling are therefore coupled manifestations of deformation and damage within the same multiphase material [1,2].

No single strength or specification index can describe resistance to all forms of asphalt distress. At high temperature, the softened mastic allows greater aggregate movement and permanent deformation. Repeated tensile strain can initiate and develop microcracks as mixture stiffness decreases. Moisture can weaken mastic cohesion and aggregate-binder adhesion, whereas aging can increase stiffness and reduce the ability of the mixture to relax stress. For this reason, the effect of a modifier should be examined under different loading and conditioning conditions rather than through one test alone.

*Corresponding author: lamya.m.mahdi@uotechnology.edu.iq
[a]orcid.org/0009-0001-4320-3460; [b]orcid.org/0009-0005-8454-8456; [c]orcid.org/0000-0002-4356-651X
DOI: http://dx.doi.org/10.17515/resm2026-2225ma0819rs

Discrete fibers can change the internal response of an asphalt mixture rather than acting only through the binder. When they are well dispersed, fibers may redistribute local stress, restrain aggregate movement, and stabilize binder-rich regions. Their effect depends on fiber geometry, dosage, dispersion, thermal stability, surface interaction, and mixture volumetrics [3]–[5]. Recent studies also show that the fiber–asphalt interface can influence mixture behavior. Pull-out strength and adhesion work have been used to study basalt-fiber/asphalt-mastic interaction [6], while comparative work on basalt, glass, and polyester fibers has related interfacial characteristics to cracking resistance [7]. These studies help explain the behavior of fiber-modified asphalt. However, surface energy, pull-out strength, and microstructure were not measured in the present study. The mechanisms discussed here are therefore used only to interpret the laboratory results.

Fiber content is therefore expected to have an optimum range rather than a continuously increasing effect. At low content, the number of fibers may be insufficient to influence many potential damage zones. At higher content, fiber–fiber contact, binder absorption or immobilization, and agglomeration may reduce coating uniformity or create nonuniform regions [5,8-11]. The 0.2%, 0.3%, and 0.4% dosages were selected from the low dosage range commonly investigated for mineral-fiber asphalt mixtures. Recent work has also examined low fiber contents and reported optimum behavior around 0.2–0.3% for its specific material system [7]. The optimum fiber content depends on the mixture and should not be considered a fixed property of the fiber.

The mixture was therefore examined under several conditions: high temperature, moisture conditioning, repeated strain, and thermal aging. Wheel tracking was used to measure permanent deformation at high temperature. Dry and conditioned tensile tests were used to compare tensile strength before and after moisture conditioning. Four-point bending was used to follow stiffness loss during repeated loading, while the Cantabro procedure was used to assess particle loss before and after thermal aging. Previous studies have also shown that the response of fiber-modified asphalt varies with temperature, moisture exposure, mixture layer, and composition [12-15].

Basalt fiber (BF) and glass fiber (GF) can be compared within the same asphalt mixture because both are mineral fibers that can tolerate normal HMA production temperatures. However, their physical and surface properties are not identical. Previous studies on BF have reported changes in Marshall properties, tensile response, moisture resistance, rutting, fracture, and fatigue at appropriate dosages [8,9,15-20]. Studies on GF have also reported improvements in cracking, rutting, and moisture-related performance [21-24]. In many published studies, however, fibers were used together with other mixture changes, such as reclaimed asphalt, diatomite, or warm-mix additives. This makes the effect of fiber type alone harder to distinguish.

Direct BF-GF comparisons made in one conventional mixture are still limited. Comparing results from separate studies is difficult because binder grade, aggregate source, gradation, volumetric properties, fiber dosage, and compaction may all be different. A fiber may also perform better in one test but show little advantage in another. For that reason, this study compares the response of the two fibers across several tests instead of judging them from one result.

This study compares 6 mm BF and GF at 0.2%, 0.3%, and 0.4% of total mixture mass in the same dense-graded HMA. The binder, aggregate, gradation, mixing procedure, and conditioning methods were kept the same for both fiber types. The mixture followed the relevant Iraqi specification for materials and gradation [25]. The study first examines the effect of dosage on Marshall and tensile response. It then compares the selected BF and GF mixtures in terms of rutting, tensile response, fatigue behavior, and particle loss.

2. Materials and Methods

2.1 Asphalt Binder

The asphalt binder was obtained from the Al-Daurah refinery and had a penetration grade of 60/70. Table 1 lists its measured physical properties.

Table 1. Physical properties of the 60/70 penetration-grade asphalt binder

Property (unit)	Standard	Result	SCRB limit
Penetration, 25 °C (0.1 mm)	ASTM D5	65	60–70
Ductility, 25 °C (cm)	ASTM D113	128	>100
Flash point (°C)	ASTM D92	284	>232
Fire point (°C)	ASTM D92	300	–
Viscosity, 135 °C (Pa·s)	ASTM D4402	0.375	–
Viscosity, 165 °C (Pa·s)	ASTM D4402	0.125	–
Softening point (°C)	ASTM D36	49	–

2.2 Aggregate and Mineral Filler

Crushed coarse aggregate and sand were combined with limestone mineral filler. The aggregate properties are presented in Table 2. The selected gradation followed SCRB R/9 Type IIIA for dense-graded HMA [25] and remained within the specified envelope (Figure 1). Based on the sieve series, the maximum aggregate size was 19 mm and the nominal maximum aggregate size was 12.5 mm. Los Angeles abrasion was determined in accordance with ASTM C131/C131M [26].

Table 2. Physical properties of the coarse and fine aggregates

Fraction / property	Standard	Result	Limit
Coarse: Los Angeles abrasion (%)	ASTM C131	21.2	30 max.
Coarse: Na_2SO_4 soundness loss (%)	ASTM C88	3.3	12 max.
Coarse: angularity (%)	ASTM D5821	98	95 min.
Coarse: flakiness index (%)	ASTM D4791	0.91	10 max.
Coarse: elongated index (%)	ASTM D4791	2.50	5 max.
Fine: bulk specific gravity	ASTM C128	2.618	–
Fine: apparent specific gravity	ASTM C128	2.625	–
Fine: water absorption (%)	ASTM C128	0.19	–
Fine: sand equivalent (%)	ASTM D2419	89.7	45 min.
Fine: deleterious material (%)	ASTM C142	1.11	3 max.

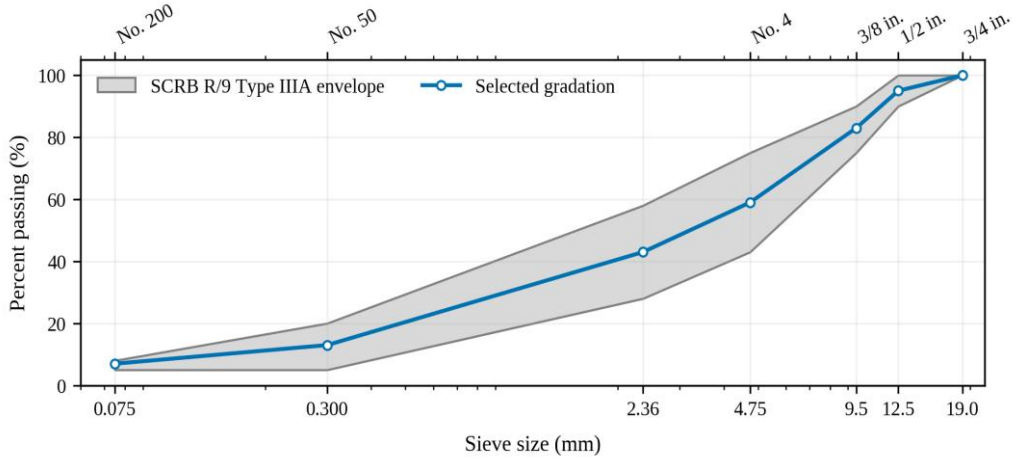

Fig. 1. Selected aggregate gradation within the SCRB R/9 Type IIIA envelope

2.3 Fibers

Basalt and glass fibers with a nominal length of 6 mm were used as received after oven drying; no additional surface treatment was applied. Their supplier-reported properties are listed in Table 3, and their physical appearance is shown in Figure 2. These values are treated as nominal constituent properties rather than measurements made in this study.

Table 3. Nominal physical and mechanical properties of the fibers

Property	Basalt fiber	Glass fiber
Length (mm)	6	6
Diameter (μm)	16	12
Density (g/cm^3)	2.77	2.60
Moisture content (%)	0.32	0.50
Elongation (%)	1.4	3.0
Tensile strength (MPa)	2,200–2,500	3,100
Elastic modulus (GPa)	87	81

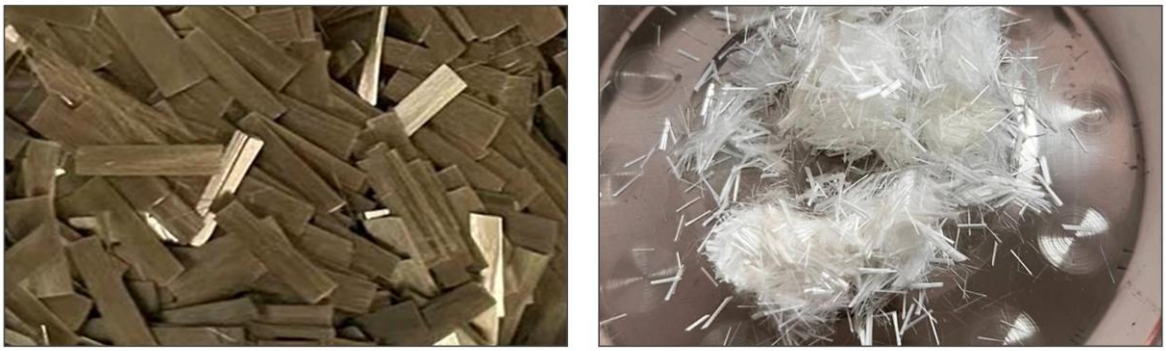

Fig. 2. Basalt fiber (left) and glass fiber (right) used in the study

2.4 Mixture Design and Specimen Preparation

The control and fiber-modified mixtures were prepared at the same asphalt content of 5.0% by total mixture mass so that fiber type and dosage could be compared under a common mixture condition. Marshall specimens were compacted with 75 blows per face in accordance with ASTM D6926 [27]. Both fibers were evaluated at 0.2%, 0.3%, and 0.4% by total mixture mass.

Before mixing, the fibers were dried at 105 °C for 24 h. A dry mixing procedure was used for both fiber types, consistent with the general approach reported for fiber-reinforced asphalt mixtures [15], [28]. For the fiber mixtures, the fibers were added first to the heated aggregate and spread through the aggregate to reduce clumping. The asphalt binder was then introduced and mixing continued. The entire mixing process took approximately 5 minutes. Mixing and compaction were carried out at approximately 153 °C and 146 °C, respectively, according to the binder viscosity–temperature relationship. Fiber distribution was checked during mixing by visual inspection, and no visible fiber balls or clumps were found. The control mixture was prepared using the same temperature and compaction sequence but without fiber.

Table 4 gives the measured volumetric properties for the control and fiber mixtures. As fiber content increased, Gmb showed a small decrease, while Va and VMA increased and VFA decreased. At the same dosage, these changes were slightly greater for BF than for GF.

Table 4. Volumetric properties of the control and fiber-modified mixtures

Mixture	Gmb (g/cm^3)	Va (%)	VMA (%)	VFA (%)
Control	2.350	4.2	15.0	72.0
0.2% BF	2.345	4.4	15.3	71.2
0.3% BF	2.340	4.6	15.6	70.5
0.4% BF	2.333	4.9	16.0	69.4
0.2% GF	2.347	4.3	15.2	71.7
0.3% GF	2.343	4.5	15.4	70.8
0.4% GF	2.338	4.7	15.7	70.1

2.5 Marshall Stability and Flow

Marshall stability and flow were measured according to ASTM D6927 [29] at a loading rate of 50.8 mm/min. Marshall quotient (MQ) was calculated using Eq. (1) and used as an empirical load-to-deformation index.

$$MQ = Marshall\ stability\ (kN) \,/\, Marshall\ flow\ (mm) \quad (1)$$

Where: MQ is the Marshall quotient (kN/mm), Marshall stability is the maximum measured load (kN), and Marshall flow is the corresponding deformation (mm).

2.6 Indirect Tensile Strength and Moisture Conditioning

Indirect tensile strength (ITS) was determined at 25 °C using ASTM D6931 [30] at a diametral loading rate of 50.8 mm/min. Moisture susceptibility was evaluated using AASHTO T283 [31]. Six specimens were prepared per mixture at 7 ± 1% air voids: three were tested unconditioned and three were vacuum-saturated, frozen at −18 ± 3 °C for 16 h, conditioned in water at 60 °C for 24 h, and equilibrated at 25 °C for 1 h. ITS was calculated using Eq. (2). Tensile strength ratio (TSR) was calculated using Eq. (3).

$$ITS = 2000P \,/\, (\pi Dt) \quad (2)$$

Where: P is peak load (N), D is specimen diameter (mm), and t is specimen thickness (mm).

$$TSR\ (\%) = (ITSconditioned \,/\, ITSunconditioned) \times 100 \quad (3)$$

Where: ITSconditioned is the indirect tensile strength of the conditioned specimens (kPa), and ITSunconditioned is the indirect tensile strength of the unconditioned specimens (kPa).

2.7 Wheel Tracking

The control, 0.3% BF, and 0.3% GF mixtures were tested according to BS EN 12697-22 [32]. Three roller-compacted slabs (400 × 300 × 50 mm) were prepared per mixture (n = 3), conditioned at 60 °C for 2 h, and tested in air at 60 °C under an approximately 700-N wheel load for 10,000 passes or until 20-mm rut depth. Rut depth was recorded with loading, and the wheel-tracking response was reported as a function of the number of passes.

2.8 Four-Point Bending Fatigue

Repeated four-point bending followed AASHTO T321 [33]. Three roller-compacted beams were tested per mixture (n = 3). The beams had nominal dimensions of 380 × 63 × 50 mm (reported actual dimensions approximately 378 × 62 × 50 mm). Testing was performed in constant-strain mode at 20 °C, 5 Hz, and 400 με. Initial flexural stiffness was defined at cycle 100; fatigue life was the number of cycles required for stiffness to decline to 50% of its initial value.

2.9 Adapted Cantabro Abrasion

An adapted procedure based on ASTM D7064/D7064M [34] was used for the control and the two 0.3% mixtures. Although ASTM D7064/D7064M was developed for open-graded friction-course mix design, Doyle and Howard [35] evaluated the Cantabro durability test across eight dense-graded asphalt mixtures and identified mass loss as a repeatable and potentially useful comparative durability measure. Accordingly, the present application was deliberately limited to a controlled within-study comparison of cohesion and particle-loss resistance; it was not used as an OGFC acceptance criterion or as a direct predictor of field raveling. Cylindrical Marshall specimens (101.6-mm nominal diameter and 63.5-mm nominal height; reported actual height approximately 62.8 mm) were tested at 25 °C in the Los Angeles abrasion machine without steel balls for 300 revolutions at 30 rpm. Aged specimens were conditioned at 60 °C for seven days (168 h). Mass loss was calculated from the initial and final specimen masses using Eq. (4).

$$Cantabro\ mass\ loss\ (\%) = [(A_i - A_e) / A_i] \times 100 \quad (4)$$

Where: A_i is the initial specimen mass before testing (g), and A_e is the final specimen mass after testing (g).

2.10 Data and Statistical Analysis

Changes relative to the control mixture were calculated using Eqs. (5) and (6). Equation (5) was used when an increase represented improvement, whereas Eq. (6) was used when a decrease represented improvement. TSR differences were expressed in percentage points.

$$Gain\ (\%) = 100(Xfiber - Xcontrol) / Xcontrol \quad (5)$$

$$Reduction\ (\%) = 100(Xcontrol - Xfiber) / Xcontrol \quad (6)$$

Where: Xfiber is the measured response of the fiber-modified mixture, and Xcontrol is the corresponding response of the control mixture. Both variables are expressed in the same units as the response being evaluated.

Results from three replicate measurements per mixture are presented as mean ± standard deviation (SD). One-way analysis of variance (ANOVA) was used to evaluate overall differences among mixture groups, followed by Tukey's honestly significant difference (HSD) test when ANOVA was significant. Statistical significance was assessed at $\alpha = 0.05$. TSR was interpreted descriptively because it was calculated from conditioned and unconditioned ITS results.

3. Results and Discussion

3.1 Dosage-Dependent Load-Flow Response

Marshall stability displayed a non-monotonic dependence on fiber content (Figure 3). Stability increased from 10.3 kN for the control to 13.1 kN for 0.3% BF and 12.1 kN for 0.3% GF, gains of 27.2% and 17.5%. At 0.4%, the corresponding mean values declined to 12.7 and 11.9 kN. Within the tested dosage range, 0.3% therefore gave the highest mean Marshall stability for both fiber types.

Flow decreased as fiber content increased. At 0.3%, mean flow decreased from 3.4 mm for the control to 2.9 mm for BF and 3.0 mm for GF, while MQ increased from 3.03 kN/mm to 4.52 and 4.03 kN/mm. MQ increased further at 0.4% because flow continued to decrease even though mean stability had started to decline. Similar non-monotonic responses have been discussed in relation to fiber restraint, binder availability, fiber–fiber interaction, and mixture homogeneity [5], [8]–[10], [16]. These mechanisms were not measured directly in this study. Based on the measured Marshall response, 0.3% provided the best balance between stability and flow within the tested range. The overall mixture-group effects were statistically significant for Marshall stability, flow, and Marshall quotient (one-way ANOVA, $p < 0.001$ for each response).

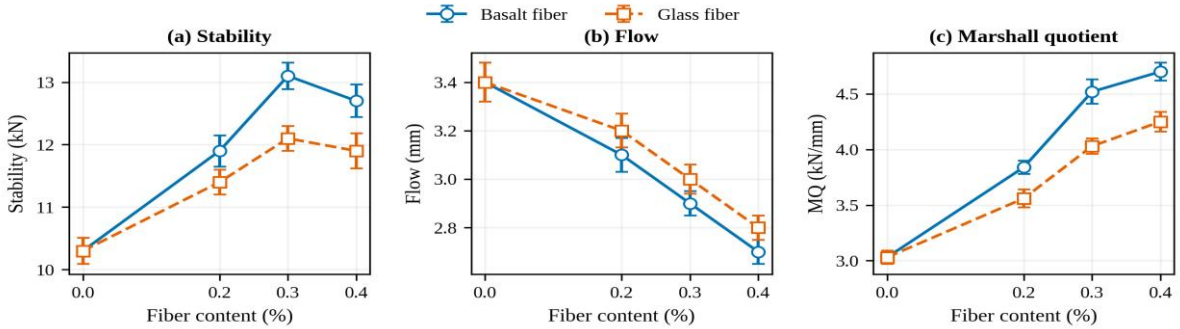

Fig. 3. Effects of basalt- and glass-fiber content on (a) Marshall stability, (b) flow, and (c) Marshall quotient. Values are means ± SD (n = 3)

3.2 Tensile Response and Moisture Conditioning

Dry and conditioned ITS followed the same non-monotonic numerical trend (Figure 4). At 0.3%, dry ITS increased from 850 kPa to 982 kPa for BF and 951 kPa for GF, whereas conditioned ITS increased from 678 kPa to 811 and 784 kPa. The corresponding gains were 15.5% and 11.9% in the dry state and 19.6% and 15.6% after conditioning. Within the tested dosage range, the highest mean dry and conditioned ITS values for both fiber types occurred at 0.3%; increasing the fiber content to 0.4% did not produce a further increase in these mean values.

TSR changed only slightly, from 80.0% for the control to 82.5% for BF and 82.5% for GF at 0.3%. The BF–GF difference was 0.0 percentage points. Thus, the two fiber mixtures had nearly the same proportional strength retention after moisture conditioning, although both had higher absolute dry and conditioned ITS values than the control. The overall mixture-group effects were statistically significant for both dry ITS and conditioned ITS (one-way ANOVA, $p < 0.001$ for each response). TSR was retained as a descriptive ratio, as specified in Section 2.10.

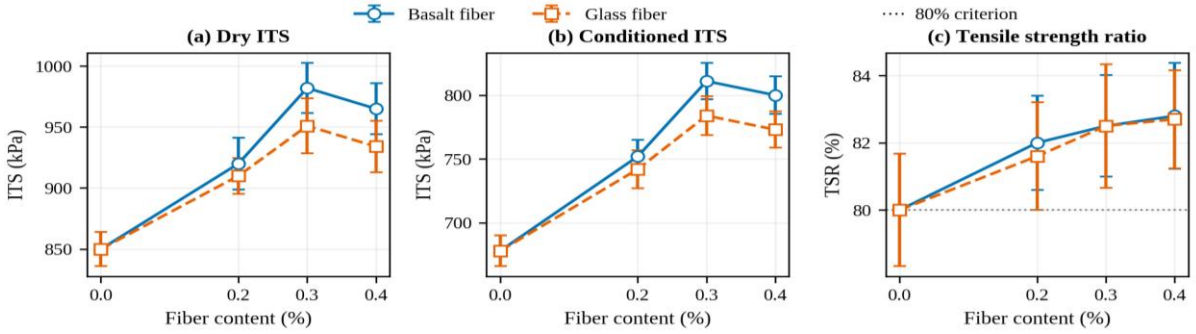

Fig. 4. Effects of fiber type and content on (a) dry ITS, (b) conditioned ITS, and (c) tensile strength ratio. Values are means ± SD (n = 3)

3.3 High-Temperature Permanent Deformation

All mixtures accumulated rut depth at 60 °C, but both fiber-modified curves remained below the control throughout the recorded loading range (Figure 5). After 10,000 passes, rut depth was 7.0 mm for the control, 4.9 mm for 0.3% BF, and 5.4 mm for 0.3% GF, corresponding to reductions of 30.0% and 22.9%, respectively (Table 5). These results show lower accumulated rut depth for the fiber-modified mixtures under the stated laboratory wheel-tracking conditions.

To characterize late-stage rut accumulation, the wheel-tracking slope (WTS) was calculated from the rut depths at 5,000 and 10,000 wheel passes shown in Figure 5 using Eq. (7). The resulting WTS values were 0.60, 0.42, and 0.46 mm/1,000 passes for the control, 0.3% BF, and 0.3% GF mixtures, respectively. These values are laboratory comparative indicators and are not field rutting-rate predictions.

$$WTS = (RD10{,}000 - RD5{,}000) / 5 \quad (7)$$

Where: WTS is the wheel-tracking slope (mm/1,000 passes), and RD5,000 and RD10,000 are the rut depths (mm) at 5,000 and 10,000 wheel passes, respectively. The BF mixture also had a higher mean MQ and initial flexural stiffness than the GF mixture. According to the supplier-reported fiber properties listed in Table 3, BF had a higher nominal modulus and a larger filament diameter than GF. These observations may help explain the lower mean rut depth of the BF mixture, but the present tests cannot separate the effects of fiber geometry, dispersion, binder absorption, and interfacial interaction. The BF–GF difference is therefore reported as a laboratory response rather than evidence of a specific microstructural mechanism [8], [15], [6], [7].

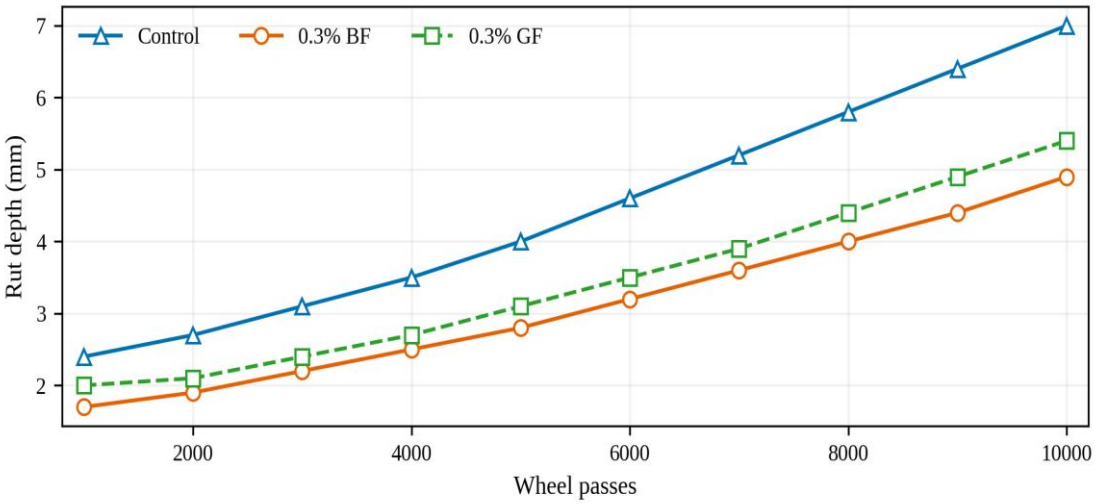

Fig. 5. Wheel-tracking response at 60 °C (n = 3 slabs per mixture)

Table 5. Wheel-tracking results and late-stage wheel-tracking slope at 60 °C

Mixture	Rut depth at 10,000 passes (mm)	Reduction vs. control (%)	WTS (mm/1,000 passes)
Control	7.0	0.0	0.60
0.3% BF	4.9	30.0	0.42
0.3% GF	5.4	22.9	0.46

3.4 Stiffness Evolution and Fatigue Damage

Initial flexural stiffness increased from 4,850 MPa for the control to 5,661 MPa for 0.3% BF and 5,431 MPa for 0.3% GF; fatigue life increased from 3,194 cycles to 4,762 and 4,674 cycles, respectively (Figure 6). These changes equal +16.7% and +12.0% in stiffness and +49.1% and +46.3% in fatigue life.

Under constant-strain loading, higher stiffness can increase the stress developed in a beam. In this study, however, both fiber mixtures showed higher mean initial stiffness and longer mean fatigue life than the control. This describes the measured response but does not identify the mechanism responsible for it. Crack bridging and interfacial effects were not measured directly and would require separate microstructural or interface testing. The mean fatigue lives of BF and GF differed by only 88 cycles, or 1.9% of the GF value. The fatigue test was conducted at one controlled strain level, 400 με, to compare the three mixtures under the same loading condition. The results therefore describe relative fatigue performance at this strain level only. They do not define a complete fatigue relationship or allow calibration of strain-dependent coefficients such as k1 and k2. Testing at several strain levels is needed for that purpose. The overall mixture-group effects were significant for initial flexural stiffness (ANOVA $p = 0.000362$) and fatigue life ($p < 0.001$). Tukey HSD showed that both fiber mixtures differed significantly from the control for both responses, whereas BF and GF did not differ significantly from each other in initial stiffness ($p = 0.1113$) or fatigue life ($p = 0.3964$).

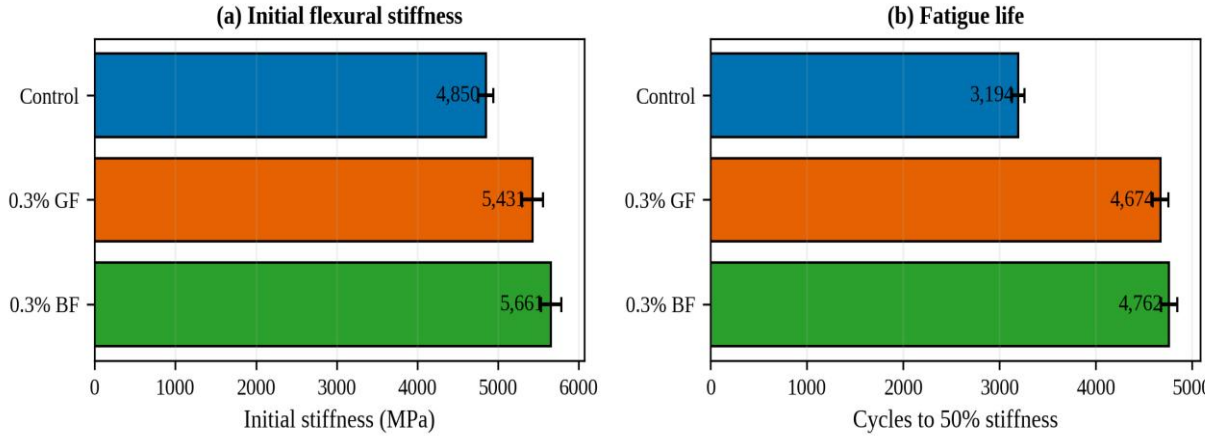

Fig. 6. Four-point bending results: (a) initial flexural stiffness and (b) fatigue life at 20 °C, 5 Hz, and 400 με. Values are means ± SD (n = 3)

3.5 Particle-Loss Resistance Before and After Aging

In the adapted Cantabro test, mean unaged mass loss decreased from 22.0% for the control to 11.3% for BF and 12.3% for GF, numerical reductions of 48.6% and 44.1% (Figure 7). After seven-day aging at 60 °C, the respective mean losses were 27.0%, 15.1%, and 18.3%; relative to the control mean, BF and GF showed reductions of 44.1% and 32.2%. Thus, under the stated adapted procedure, both fiber mixtures showed lower mean particle loss than the control, with BF giving the lowest mean loss in both conditions. Thermal aging increased mean mass loss by 5.0 percentage points for the control, 3.8 points for BF, and 6.0 points for GF. Doyle and Howard [35] also reported that the Cantabro test can differentiate among dense-graded mixtures. The relatively high absolute losses of the control (22.0% unaged and 27.0% aged) should be viewed within the conditions of this adapted test, including the fixed 5.0% binder content and the dense-graded mixture structure. Void structure and effective binder availability may affect particle retention, but their individual effects were not isolated here. For this reason, the Cantabro results are used only to compare the mixtures tested in this study and are not interpreted using OGFC acceptance limits or as direct predictions of field raveling. The overall mixture-group effects were statistically significant for Cantabro mass loss in both the unaged and aged conditions (one-way ANOVA, $p < 0.001$ for each condition).

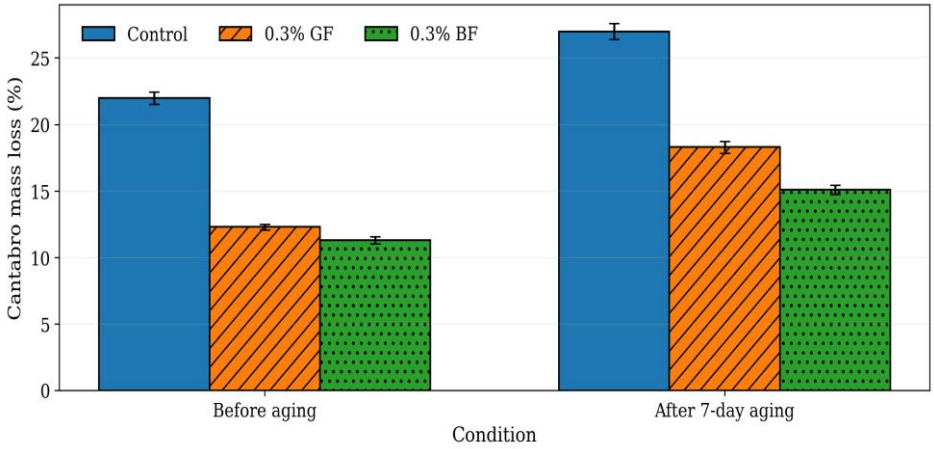

Fig. 7. Cantabro mass loss before and after seven-day aging at 60 °C under the adapted procedure. Values are means ± SD (n = 3)

3.6 Cross-Test Material-Response Synthesis

Across the measured responses, 0.3% gave the most balanced result within the tested dosage range. At 0.4%, MQ and TSR increased slightly, but mean stability and dry ITS decreased from their

0.3% values. For this reason, the selected dosage was based on the combined Marshall and tensile response rather than on the highest value of a single index.

Table 6. Descriptive effect magnitudes for the selected 0.3% mixtures relative to the control

Performance indicator	0.3% BF	0.3% GF	BF–GF contrast
Marshall stability increase (%)	+27.2	+17.5	+9.7
Marshall flow reduction (%)	+14.7	+11.8	+2.9
Dry ITS increase (%)	+15.5	+11.9	+3.6
Conditioned ITS increase (%)	+19.6	+15.6	+4.0
TSR gain (percentage points)	+2.5	+2.5	0.0
Final rut-depth reduction (%)	+30.0	+22.9	+7.1
Initial stiffness increase (%)	+16.7	+12.0	+4.7
Fatigue-life increase (%)	+49.1	+46.3	+2.8
Aged Cantabro-loss reduction (%)	+44.1	+32.2	+11.9
Unaged Cantabro-loss reduction (%)	+48.6	+44.1	+4.5

Note: Values are percentage changes unless identified as percentage points. A positive BF–GF contrast denotes the larger favorable numerical response for BF.

In this study, "performance fingerprint" means the pattern of results obtained from the different laboratory tests. It is not a weighted index or a combined score. Table 6 lists the response of each test separately. From the group means, BF had larger numerical changes than GF for several indicators, although the size of the difference depended on the test. The largest BF-GF differences were found for aged particle loss, Marshall stability, and rut depth. In contrast, TSR was the same for both fibers and the fatigue-life results were close. The term is therefore used only to describe the pattern across the tests and not to rank the two fibers statistically.

3.7 Indicative Economic Consideration

At the selected fiber content of 0.3% by total mixture mass, one ton of asphalt mixture requires approximately 3 kg of fiber. The direct additional fiber-material cost can therefore be expressed using Eq. (8):

$$\Delta C = (3\ kg/tonne)\ Cf \tag{8}$$

Where: ΔC is the additional fiber-material cost per ton of asphalt mixture and Cf is the local fiber price per kilogram. An indicative economic framework is presented because the economic value of fiber modification depends on local material, construction, maintenance, and long-term performance conditions [36]. At the present laboratory stage, the measured performance changes provide the technical basis for a future field-calibrated life-cycle evaluation. Field sections can subsequently be used to relate the additional fiber cost to maintenance demand and rehabilitation intervals under local conditions.

4. Conclusions

The tests in this study were carried out on one dense-graded HMA with 5.0% asphalt binder. Both 6 mm BF and 6 mm GF were tested at 0.2%, 0.3%, and 0.4% of total mixture mass. The Marshall and tensile results showed that 0.3% provided the most balanced response within the tested range, so this dosage was used for the additional tests. At 0.3%, mean Marshall stability increased by 27.2% for BF and 17.5% for GF. Mean dry ITS increased by 15.5% and 11.9%, respectively, and conditioned ITS also increased. The TSR value was 82.5% for both mixtures, so there was practically no numerical difference between BF and GF in moisture-strength retention.

The wheel-tracking results also showed lower rut depths for the fiber mixtures. After 10,000 wheel passes at 60 °C, the mean rut depth was 7.0 mm for the control, 4.9 mm for BF, and 5.4 mm for GF. In the four-point bending test at 20 °C, 5 Hz, and 400 με, both fiber mixtures had higher mean initial stiffness and longer mean fatigue life than the control. The results at 400 με provide a direct comparison of the three mixtures under the selected fatigue condition, while testing at additional strain levels would extend the fatigue characterization. Both fibers also reduced mean Cantabro particle loss before and after seven days of thermal aging, with BF giving the lowest mean aged loss. The adapted Cantabro procedure therefore provides a consistent comparative measure of particle-loss resistance for the dense-graded mixtures evaluated here.

Taken together, the results show that the effect of the fibers was not the same in every test. BF produced larger numerical changes in rut depth and aged particle loss, whereas BF and GF were very close in TSR and fatigue life. The two fibers should therefore be compared according to the response of interest rather than by one overall ranking. The observed laboratory improvements provide a useful basis for material selection and for subsequent field evaluation of long-term pavement performance. The present investigation focused on one 60/70 penetration-grade binder, one dense gradation, 5.0% asphalt content, laboratory conditioning, and one fatigue strain level. Future work can broaden this experimental scope through field sections, fatigue testing at several strain levels, low-temperature cracking tests, microstructural and interface characterization, and life-cycle cost analysis using documented local costs and field performance data.

References

[1] Huang YH. Pavement Analysis and Design. 2nd ed. Upper Saddle River, NJ: Pearson Prentice Hall; 2004.
[2] Read J, Whiteoak D. The Shell Bitumen Handbook. 6th ed. London: ICE Publishing; 2015.
[3] Abtahi SM, Sheikhzadeh M, Hejazi SM. Fiber-reinforced asphalt-concrete-A review. Construction and Building Materials. 2010;24(6):871-877. https://doi.org/10.1016/j.conbuildmat.2009.11.009
[4] Slebi-Acevedo CJ, Lastra-González P, Pascual-Muñoz P, Castro-Fresno D. Mechanical performance of fibers in hot mix asphalt: A review. Construction and Building Materials. 2019;200:756-769. https://doi.org/10.1016/j.conbuildmat.2018.12.171
[5] Guo Y, Tataranni P, Sangiorgi C. The use of fibres in asphalt mixtures: A state-of-the-art review. Construction and Building Materials. 2023;390:131754. https://doi.org/10.1016/j.conbuildmat.2023.131754
[6] Wu B, Pei Z, Xiao P, Lou K. Evaluation of the interfacial interaction ability between basalt fibers and the asphalt mastic. Materials. 2022;15(22):8209. https://doi.org/10.3390/ma15228209
[7] Tang Q, Xiao P, Lou K, Wu Y. Interfacial characteristics of fiber asphalt mastic and aggregates: Impact on mixture crack resistance performance. Construction and Building Materials. 2024;414:134866. https://doi.org/10.1016/j.conbuildmat.2024.134866
[8] Zhao H, Guan B, Xiong R, Zhang A. Investigation of the performance of basalt fiber reinforced asphalt mixture. Applied Sciences. 2020;10(5):1561. https://doi.org/10.3390/app10051561
[9] Lou K, Xiao P, Kang A, Wu Z, Li B, Lu P. Performance evaluation and adaptability optimization of hot mix asphalt reinforced by mixed lengths basalt fibers. Construction and Building Materials. 2021;292:123373. https://doi.org/10.1016/j.conbuildmat.2021.123373
[10] Serin S, Onal Y, Emiroglu M, Demir E. Comparison of the effect of basalt and glass fibers on the fracture energy of asphalt mixes using semi-circular bending test. Construction and Building Materials. 2023;406:133460. https://doi.org/10.1016/j.conbuildmat.2023.133460
[11] Shi C, Wang J, Sun S, Guan C. Research on basalt fiber oil/asphalt absorption performance and test methods suitable for asphalt mixture with different structures. Coatings. 2024;14(2):204. https://doi.org/10.3390/coatings14020204
[12] Mt Rodhi MS, Mahmud MZH, Abdul Hassan N, Ab Aziz Z, Jaya RP, Batun SN, Al Dulaimi HRR. Laboratory evaluation of basalt fiber-reinforced dense-graded asphalt. Malaysian Journal of Civil Engineering. 2026;38(2):149-161. https://doi.org/10.11113/mjce.v38.26487
[13] Riccardi C, Indacoechea I, Wang D, Lastra-González P, Cannone Falchetto A, Castro-Fresno D. Low-temperature performance of fiber-reinforced asphalt mixtures for surface, binder, and base layers. Cold Regions Science and Technology. 2023;206:103738. https://doi.org/10.1016/j.coldregions.2022.103738
[14] Mohd Asri MAA, Mohd Warid MN, Kamarudin SNN, Hainin MR. Fibre glass in asphalt: A review of current trends in durability and performance. Next Research. 2026;6:101402. https://doi.org/10.1016/j.nexres.2026.101402
[15] Hui Y, Men G, Xiao P, Tang Q, Han F, Kang A, Wu Z. Recent advances in basalt fiber reinforced asphalt mixture for pavement applications. Materials. 2022;15(19):6826. https://doi.org/10.3390/ma15196826

[16] Morova N. Investigation of usability of basalt fibers in hot mix asphalt concrete. Construction and Building Materials. 2013;47:175-180. https://doi.org/10.1016/j.conbuildmat.2013.04.048
[17] Celauro C, Praticò FG. Asphalt mixtures modified with basalt fibres for surface courses. Construction and Building Materials. 2018;170:245-253. https://doi.org/10.1016/j.conbuildmat.2018.03.058
[18] Lou K, Wu X, Xiao P, Zhang C. Investigation on fatigue performance of asphalt mixture reinforced by basalt fiber. Materials. 2021;14(19):5596. https://doi.org/10.3390/ma14195596
[19] Cheng Y, Yu D, Gong Y, Zhu C, Tao J, Wang W. Laboratory evaluation on the performance of eco-friendly basalt fiber and diatomite compound modified asphalt mixture. Materials. 2018;11(12):2400. https://doi.org/10.3390/ma11122400
[20] Wang W, Cheng Y, Ma G, Tan G, Sun X, Yang S. Further investigation on damage model of eco-friendly basalt fiber modified asphalt mixture under freeze-thaw cycles. Applied Sciences. 2019;9(1):60. https://doi.org/10.3390/app9010060
[21] Morea F, Zerbino R. Improvement of asphalt mixture performance with glass macro-fibers. Construction and Building Materials. 2018;164:113-120. https://doi.org/10.1016/j.conbuildmat.2017.12.198
[22] Fakhri M, Hosseini SA. Laboratory evaluation of rutting and moisture damage resistance of glass fiber modified warm mix asphalt incorporating high RAP proportion. Construction and Building Materials. 2017;134:626-640. https://doi.org/10.1016/j.conbuildmat.2016.12.168
[23] Guo Q, Li L, Cheng Y, Jiao Y, Xu C. Laboratory evaluation on performance of diatomite and glass fiber compound modified asphalt mixture. Materials & Design. 2015;66:51-59. https://doi.org/10.1016/j.matdes.2014.10.033
[24] Ziari H, Aliha MRM, Moniri A, Saghafi Y. Crack resistance of hot mix asphalt containing different percentages of reclaimed asphalt pavement and glass fiber. Construction and Building Materials. 2020;230:117015. https://doi.org/10.1016/j.conbuildmat.2019.117015
[25] State Corporation for Roads and Bridges. Standard Specifications for Roads and Bridges, Section R/9: Hot-Mix Asphalt Concrete Pavement. Baghdad: Ministry of Housing and Construction, Republic of Iraq; 2003.
[26] ASTM International. ASTM C131/C131M-20: Standard Test Method for Resistance to Degradation of Small-Size Coarse Aggregate by Abrasion and Impact in the Los Angeles Machine. West Conshohocken, PA: ASTM International; 2020.
[27] ASTM International. ASTM D6926-20: Standard Practice for Preparation of Asphalt Mixture Specimens Using Marshall Apparatus. West Conshohocken, PA: ASTM International; 2020.
[28] Mrema AH, Noh SH, Kwon OS, Lee JJ. Performance of glass wool fibers in asphalt concrete mixtures. Materials. 2020;13(21):4699. https://doi.org/10.3390/ma13214699
[29] ASTM International. ASTM D6927-22: Standard Test Method for Marshall Stability and Flow of Asphalt Mixtures. West Conshohocken, PA: ASTM International; 2022.
[30] ASTM International. ASTM D6931-17: Standard Test Method for Indirect Tensile (IDT) Strength of Bituminous Mixtures. West Conshohocken, PA: ASTM International; 2017.
[31] AASHTO. AASHTO T 283: Standard Method of Test for Resistance of Compacted Asphalt Mixtures to Moisture-Induced Damage. Washington, DC: AASHTO; 2016.
[32] British Standards Institution. BS EN 12697-22:2020, Bituminous Mixtures-Test Methods-Part 22: Wheel Tracking. London: BSI; 2020.
[33] AASHTO. AASHTO T 321: Determining the Fatigue Life of Compacted Asphalt Mixtures Subjected to Repeated Flexural Bending. Washington, DC: AASHTO; 2017.
[34] ASTM International. ASTM D7064/D7064M-08(2013): Standard Practice for Open-Graded Friction Course (OGFC) Mix Design. West Conshohocken, PA: ASTM International; 2013.
[35] Doyle JD, Howard IL. Evaluation of the Cantabro durability test for dense graded asphalt. Geo-Frontiers 2011: Advances in Geotechnical Engineering, GSP 211, Dallas, TX; 2011:4563-4572. https://doi.org/10.1061/41165(397)467
[36] Fahad M, Richard N. Cost efficiency evaluation of ceramic fiber, glass fiber, and basalt fiber-reinforced asphalt mixtures. Applied Sciences. 2025;15(14):7919. https://doi.org/10.3390/app15147919